This article has been accepted for publication in a future issue of this journal, but has not been fully edited. Content may change prior to final publication. Citation information: DOI 10.1109/JIOT.2022.3141402, IEEE Internet of Things Journal

Dynamic Detection Based Trajectory Planning for Autonomous Underwater Vehicle to Collect Data From Underwater Sensors

Mingyue Cheng, *Graduate Student Member, IEEE*, Quansheng Guan, *Senior Member, IEEE*, Fei Ji, *Member, IEEE*, Julian Cheng, *Senior Member, IEEE*, and Yankun Chen

***Abstract*—Marine science and Internet of underwater things applications rely significantly on collecting data from underwater sensors. Data collection using long-distance underwater acoustic communications consumes a lot of energy in underwater sensor nodes, which are powered by batteries. To achieve low-energy consumption, we can use the autonomous underwater vehicle (AUV) to move close to sensor nodes and exploit the short-range and high-rate communications. Most of the existing AUV-based data collection schemes consider the scenarios having the knowledge of node positions, where the cruising trajectory can be computed before the AUV's departure. These schemes cannot apply to some scenarios such as turtle tracking for a certain sea area having no position information. To this end, we first propose a planning-while-detecting approach to dynamically detect the sensors on turtles and adjust the AUV cruising direction to collect data. To further improve data efficiency under the energy limit of the AUV, we group the sensors that can share the same trajectory using their detected directions. A grouping-based dynamic trajectory planning (GDTP) is then proposed to determine the next cruising direction that can visit the group of sensors having the largest amount of data and demanding the least cruising energy at the risk of detection errors. Simulation results show that GDTP achieves significantly higher data collection efficiency than the existing trajectory planning algorithms in dynamic scenarios, and as the communication range increases, it can even outperform existing algorithms with node locations.**

***Index Terms*—Internet of Underwater Things (IoUT), data collection, autonomous underwater vehicle (AUV), dynamic trajectory planning, node detection.**

I. Introduction

The ocean covers more than 70% of the earth, while only five percent of the ocean has been explored by humans. The under-explored ocean has attracted increasing attention and interests of human beings. Recent development in data science has introduced a new paradigm in marine research to obtain more knowledge of the ocean [1]. Therefore, data acquisition has become more important than ever for marine science and Internet of Underwater Things (IoUT) applications [2].

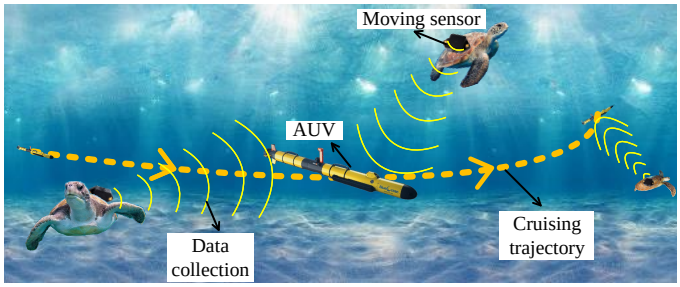

Fig. 1. An IoUT application example. The AUV collects tracking data on sea turtles.

The IoUT applications rely on deploying underwater sensors to sense underwater environmental parameters (e.g., temperature, salt, depth, acoustic Doppler current profiler, etc.). Two basic approaches can be used to collect data from the sensors wirelessly. One approach is to allow the sensors to report their data to the sink on the water surface directly or via multi-hop forwarding [3]. However, the long distance between the sensor and the sink requires high-power underwater acoustic communications, which will deplete the limited battery in the sensors fast. Another approach uses an autonomous underwater vehicle (AUV) to collect data from the underwater sensors [4]. The AUV can move close to a sensor node, and then collect and relay the collected data via short-range and high-rate radio-frequency (RF) or optical links. The relaying by AUVs can reduce the energy consumption of underwater sensor nodes, since underwater acoustic communications are energy-consuming for the battery-powered underwater sensor nodes.

Trajectory planning is the key to AUV-based data collection approaches. Traditionally, the AUV is designed to cruise along a fixed trajectory, such as layered-scan paths [5], linear round-trip trajectory [6], ellipse trajectory [7], [8], [9], spiral trajectory [10], [11]. In order to traverse all the sensor nodes and collect the data therein, a static trajectory can be carefully calculated based on node positions before deploying the AUV [5], [12], [13], [14], [15].

However, the positions of underwater sensor nodes are unavailable in some IoUT applications. Take the turtle tracking

This work was supported by the National Natural Science Foundation of China under Grants 62192712 and U1801261, the Guangdong Provincial Key Laboratory of Short-Range Wireless Detection and Communication under Grant 2017B030314003, and key-area research and development program of Guangdong Province under Grant 2020B0101130023.

Mingyue Cheng, Quansheng Guan, and Fei Ji are with School of Electronic and Information Engineering, South China University of Technology, Guangzhou, 510640, China, and also with Key Laboratory of Marine Environmental Survey Technology and Application, Ministry of Natural Resources, Guangzhou, 510300, China. (Corresponding author: Quansheng Guan; e-mail: eeqshguan@scut.edu.cn)

Julian Cheng is with the School of Engineering, University of British Columbia, Kelowna, BC, Canada.

Yankun Chen is with the South China Sea Marine Survey and Technology Center, State Oceanic Administration, Guangzhou, 510300, China, the Key Laboratory of Marine Environmental Survey Technology and Application, Ministry of Natural Resources Guangzhou, 510300, China, and also with the Southern Marine Science Engineering Guangdong Laboratory Zhuhai, 440402, China.

in Fig. turtle as an example, where the sensors are mounted on the turtles to track their underwater migration route. The short-range relay based data collection by the AUV can significantly prolong the lifetime of sensors on turtles. However, it is impossible to compute a static trajectory for the AUV with unknown positions, since the turtles are moving. Even though the sensors are fixed, we cannot know the exact coordinates of the sensors since there is no positioning system underwater, which is different from terrestrial Internet of Things (IoT) systems.

Without the positions of moving nodes, it is challenging to plan a dynamic trajectory. The AUV has to detect the existence of the nearby sensors and adjust its cruise trajectory based on the detection information dynamically. Due to the large sea area and signal attenuation, the AUV can detect only the nearby sensor nodes and limited information (e.g., the direction of the sensor nodes) is available. Considering also the limited cruising energy of the AUV, it is difficult to design a data-efficient dynamic path for the AUV.

To address the above challenges for the dynamic trajectory planning based data collection, we propose a planning-while-detecting framework, where the long-propagation acoustic waves are used to detect and estimate the existence of sensor nodes. Besides, the short-range communications are used for data transmissions between the AUV and the sensor nodes. Before the energy is exhausted, the AUV floats to the surface and delivers the collected data to a sink.

The main contributions to this paper are summarized as follows:

- *Planning-while-detecting:* To address the position unavailability, we propose a planning-while-detecting framework, which formulates the dynamic cruising adjustment as an expected payoff maximization problem considering the gain of the collected data from sensors, the cost of the AUV movement, and the data loss in the unvisited nodes based on the detected directions and detection probabilities of sensors. Individual-based dynamic trajectory planning (IDTP) is proposed to dynamically visit the next sensor having the maximum payoff.
- *Grouping-based dynamic trajectory planning (GDTP):* To further improve data efficiency under the limited energy of the AUV, we group the sensors that can share a common communication area of the trajectory using their detected directions, such that one movement of the AUV can collect a group's data. A grouping-based dynamic trajectory planning (GDTP) is then proposed to determine the next cruising direction that can visit the group of sensors having the largest amount of data and demanding the least cruising energy under detection uncertainty.

The remainder of this paper is arranged as follows. Section II reviews the related work in AUV data collection. In Section III, we present the system model and formulate the data collection problem. Then we present the proposed GDTP algorithm in Section IV. Section V shows and discusses the simulation results. Finally, Section VI concludes this paper.

II. Related Work

In the literature and the practical applications, there are three kinds of path planning for AUV-based data collection: fixed path, static path, and dynamic path.

A. Fixed Path Planning

The fixed planning does not require the node information, and the AUV just traverses the entire or part of the area along a fixed and pre-defined path.

Without the knowledge of node positions, the fixed path planning is proposed to scan the monitored sea area and collect the data. Inspired by the lawn mower pattern, the reference [16], [17] proposed a z-shaped path to traverse sensors at the same depth. Han *et al.* extended the fixed z-shaped path to three-dimensional underwater acoustic sensor networks (UASNs) by proposing a grid and probabilistic neighborhood-based data collection algorithm with layered-scan (GPN-LSCAN) [5].

The energy of AUV is limited to scan a large monitoring sea area. To this end, Ilyas *et al.* proposed an AUV-aided efficient data gathering (AEDG) routing protocol [8], where the AUV moves along a fixed elliptical trajectory. The AEDG shortens the journey of the trajectory by allowing sensors far from the elliptical trajectory to deliver their data to a node near the trajectory via multiple hops. Similarly, Han *et al.* proposed a fixed spiral trajectory for the AUV. Since the multi-hop data forwarding may make the nodes near the trajectory become the communication hot spots, the reference [11] proposed a multi-AUV scheme to release the hot spots.

B. Static Path Planning

Static path planning calculates a cruising trajectory according to the positions of sensor nodes before the departure of the AUV. Therefore, static path planning is often applied to the case where the sensor deployment is fixed and the node positions are known in advance.

Static planning to traverse all the sensor nodes with limited energy of AUV is similar to the classic traveling salesman problem (TSP) and is often NP-hard. Taking the static planning as a TSP, a nearest-neighbor (N-n) algorithm [18] was proposed to always visit the closest neighbor from the current location.

To reduce the number of nodes that the AUV has to traverse, many algorithms have been proposed to cluster the sensor nodes, and only cluster headers need to be traversed [13], [5], [14], [19]. Han *et al.* proposed a probabilistic neighborhood covering set-based greedy heuristic algorithm (PNCS-GHA) [5], which constructs a minimum probabilistic neighborhood covering set (PNCS) to divide nodes into clusters and shorten the length of the cruise journey. Duan *et al.* used the value of information (VoI) of the data as the criterion to divide the network into several clusters [14], where a static path is calculated to visit the cluster with the largest VoI.

This article has been accepted for publication in a future issue of this journal, but has not been fully edited. Content may change prior to final publication. Citation information: DOI 10.1109/JIOT.2022.3141402, IEEE Internet of Things Journal

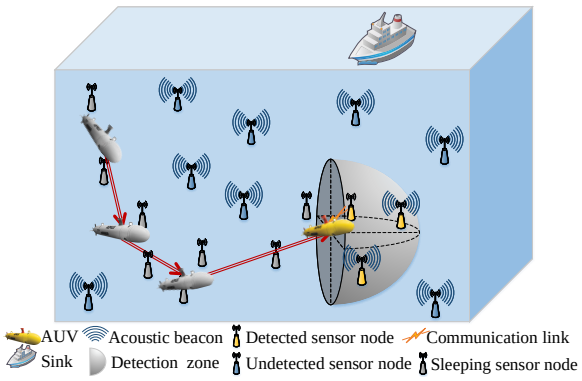

Fig. 2. An example of network model. The AUV detects the existence of sensor nodes during its cruise, moves close to sensor nodes, and collects their data.

C. Dynamic Path Planning

When the node positions are not available in advance, prior static path planning cannot be calculated for the AUV. In this case, the AUV has to determine its ongoing trajectory dynamically during its journey.

Basagni *et al.* proposed a greedy and adaptive AUV path planning (GAAP) based on VoI [20]. In this paper, the VoI is defined as a decreasing function of time. Whenever the new data is generated, the sensor node transmits a short packet through the acoustic channel to the AUV to report VoI. According to the received VoI information, the AUV adjusts its trajectory dynamically to maximize the VoI of the data delivered to the sink.

To reduce the cruising journey and save energy of the AUV, Yan *et al.* proposed an energy-efficient data collection solution (EDCS) for AUV-assisted UASN [21]. EDCS allows nodes to transmit their data to gateways, and the AUV just needs to visit the gateways node and uses a short cruising path to maximize VoI of the collected data. However, the existing dynamic trajectory planning relies on the knowledge of node positions, and adjusts the AUV's trajectory based on the reported VoI in the communication range, but not the detected information from sensor nodes.

Dynamic trajectory planning is also used to avoid underwater obstacles for the AUV. Lv *et al.* proposed to dynamically adjust the AUV cruising by predicting the obstacle's trajectory and analyzing the probability of collision to achieve safe obstacle avoidance [22]. However, the obstacle avoidance differs significantly from the data collection without node positions.

III. System Model and Problem Formulation

A. Network Architecture

We consider the data collection in an underwater sensor network, where sensor nodes are deployed in a three-dimensional underwater environment with a size of $L \times W \times H$, as shown in Fig. 2. The sink is located on the surface of the water area. An AUV is cruising in the water and tries to visit the underwater sensor nodes to collect the sensed data. In this case, the AUV and the visited sensor nodes can exploit the short-range high-speed communication technologies [1] for the data transmissions, as shown in Fig. 2. Usually, short-range communications consume less energy than long-range communications due to signal attenuation [24]. Thus, short-range communications can save the energy of the underwater sensor nodes and prolong the lifetime of the network.

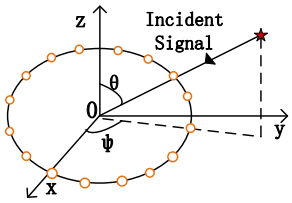

Fig. 3. The AUV uses the UCA to detect the angles of the incident signal.

B. Sensor Node Model

We consider the case that the positions of the underwater sensor nodes are unavailable. The AUV has to detect the underwater sensor nodes and plan its cruising path dynamically to collect data. To achieve node detection for the AUV, we enable the sensor nodes to periodically broadcast underwater acoustic beacons to show their existence. The sensor node broadcasts beacons when its sensed data reaches to B bytes; otherwise, the transmitter will keep silent to save energy. After transmitting the data to the AUV, the sensor nodes will empty their buffers and start a new round of sensing, as shown in Fig. 2.

C. AUV Model

The AUV is equipped with a uniform circular array (UCA) to receive the beacon signals and detect the existence of sensor nodes in the 3-dimensional underwater environment. The UCA contains M elements and estimates the azimuth angle φ and the pitch angle θ of the incident signal as shown in Fig. 3, where O is the position of the AUV. Suppose there are K ($K \leq M-1$) signals incident on the array and each signal $s_k(t)(k = 1, 2, \cdots, K)$ is from the direction $(\theta_k, \varphi_k)(k = 1, 2, \cdots, K, -\frac{\pi}{2} < \theta_k < \frac{\pi}{2}, -\frac{\pi}{2} < \varphi_k < \frac{\pi}{2})$. At time t, the received signals $\mathbf{X}$ of the UCA can be expressed as [25], [26]

$$\mathbf{X} = \boldsymbol{A}(\theta, \varphi)\mathbf{S}(t) + \mathbf{N}(t), \tag{1}$$

where, $\mathbf{S}(t) = [s_1(t), s_2(t), \cdots, s_K(t)]^{\mathrm{T}}$ represents the received signal vector, $\mathbf{N}(t) = [n_1(t), n_2(t), \cdots, n_M(t)]^{\mathrm{T}}$ represents the noise vector, and $\boldsymbol{A}$ denotes the steering matrix. The steering matrix for the UCA is

$$\boldsymbol{A}(\theta, \varphi) = [\boldsymbol{a}_1, \boldsymbol{a}_2, \cdots, \boldsymbol{a}_K], \tag{2}$$

[1]For example, underwater acoustic communications can reach 1.2 Mbps over a distance of 12 meters with tens of watts power [23], underwater optical communications can reach Gbps with a transmission power of several watts within a range of 10 to 100 meters [24], and underwater RF communications can reach Mbps at about 10 meters with a transmission power of a few milliwatts to 100 watts [24].

where

$$\boldsymbol{a}_i = \begin{bmatrix} \exp(-j2\pi R\sin\theta_i\cos(\varphi_i-\phi_0)/\lambda) \\ \exp(-j2\pi R\sin\theta_i\cos(\varphi_i-\phi_1)/\lambda) \\ \cdots \\ \exp(-j2\pi R\sin\theta_i\cos(\varphi_i-\phi_{M-1})/\lambda) \end{bmatrix}, \quad (3)$$

$\phi_k = 2\pi m/M(m = 0, 1, \cdots, M-1)$ and R denotes the radius of the UCA, and λ represents the wavelength.

Since a UCA with M elements can resolve at most $M-1$ sources, let the first K incident angles represent the incident directions of the real signal sources, and the last $(M-1-K)$ incident angles are the incident directions of the virtual signal sources generated by noises. When there is no noise, the waveform of the virtual signal source satisfies $s_k(t) = 0$, for $k = M-1-K, ..., M-1$. Eq. (1) can be rewritten as

$$\mathbf{X}(t) = \sum_{k=1}^{K} \boldsymbol{a}_k s_k(t) + \sum_{k=K+1}^{M-1} \boldsymbol{a}_k s_k(t) + \mathbf{N}(t). \quad (4)$$

Through the calculation and processing of the received signals, the directions of $(M-1)$ signals are estimated. In order to distinguish whether the signal in the estimated direction $(\hat{\theta}_i, \hat{\varphi}_i)$ comes from a possible node or is a virtual signal, the power likelihood ratio hypothesis test is used [27]. Theoretically, the power of the k-th node can be expressed as

$$p_k = \frac{1}{N}\sum_{n=1}^{N}|s_k(n)|^2 + \sigma^2, \quad (5)$$

where $s_k(t)$ is the k-th signal source waveform, σ^2 represents noise variance, and N is the snapshots number. The hypothesis test for the signal power of the estimated incident direction $(\hat{\theta}_k, \hat{\varphi}_k)$ is

$$\begin{aligned} &H_0(k) : \hat{p}_k = \sigma^2, \\ &H_1(k) : \hat{p}_k = (M-1)p_k + \sigma^2. \end{aligned} \quad (6)$$

The H_1 judgment is made in $(\hat{\theta}_k, \hat{\varphi}_k)$, towards which direction there is a node b_k with a detection probability P_k^D. If the decision is H_0, the direction $(\hat{\theta}_k, \hat{\varphi}_k)$ contains only noises. The details of the angle estimation and the calculation for the detection probability will be specified in Section IV-A. The notions used in our study are listed in Tab. I.

D. Problem Formulation

Multiple nodes in multiple directions may be detected, leading to multiple choices of decisions on cruising. The cruising decisions are expressed as different branches in Fig. 4. For each node, the AUV has two options "visit" and "not visit".

The AUV has to consider the following cases before its next cruising:

- The visit of a node can collect the data therein and obtains a positive payoff. However, the node detection may experience errors and false alarms. When the AUV chooses to visit a node, there may be no nodes in that cruising direction. Thus, the cruising energy is wasted in such a case, and the AUV will receive a negative payoff.

TABLE I
NOTATIONS

Notation	Definition
$\mathcal{P}$	The cruise path of the AUV
$\mathcal{P}_i$	The i-th hover point of the AUV
$\mathcal{B}$	The set of detected nodes
B	The size of the node's data
b_i	The detected node i
θ_i	The azimuth angle of b_i
φ_i	The pitch angle of b_i
P_i^D	The detection probability of b_i
$\mathcal{L}(\cdot)$	The travel cost of the AUV from the current hover position
D	The detection range of the AUV
C	The communication range of the AUV and sensors
$u_v(b_i)$	The expected payoff of visiting b_i
$u_n(b_i)$	The expected payoff of not visiting b_i
E_{ini}	Initial energy carried by the AUV
E_{rel}	The current residual energy of the AUV
E_{back}	The energy for the AUV to return to sink from next hover point
M	The number of hydrophone elements in UCA
σ^2	Noise variance
p_k	The k-th source's received signal power at the UCA

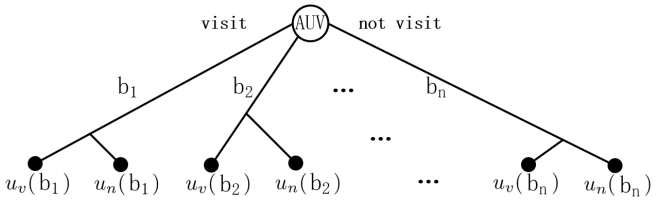

Fig. 4. The payoff extended form of the AUV

- When the AUV chooses to visit a node, the remaining nodes cannot be visited. Thus, the sensed data in those nodes will be lost, which means a negative payoff for data collection.

Assuming that each node contains B bytes of data. Thus, the collection of B bytes' data will obtain a payoff of B. The cost is the energy consumption of the AUV movement. Suppose the sound waves emitted by the nodes diffuse in a spherical manner, the detection area of the AUV is a hemisphere with a radius D. This radius represents the farthest distance at which a node can be detected. Once the AUV decides its cruising direction, it will move to a hover point which is within the communication range of that node to collect data. Let $\mathcal{L}_0$ be the energy consumption for an AUV movement of one meter. Considering that the detection probability for a node relates to the distance between that node and the AUV, the cruising cost of visiting a node b_i from the current hover position can be given by

$$\mathcal{L}(b_i) = \mathcal{L}_0 \cdot D \cdot \exp(-\frac{\mathrm{P}_i^D}{1-\mathrm{P}_i^D}). \quad (7)$$

The cruise cost of the AUV moving to the detection edge is defined as $\mathcal{L}_c = \mathcal{L}_0 \cdot D$. The payoff matrix of the AUV cruising decisions is summarized in Tab. II. According to the payoff matrix, the expected payoff $u_v(b_i)$ for visiting b_i and the

This article has been accepted for publication in a future issue of this journal, but has not been fully edited. Content may change prior to final publication. Citation information: DOI 10.1109/JIOT.2022.3141402, IEEE Internet of Things Journal

TABLE II
THE PAYOFF MATRIX OF THE AUV CRUISING DECISIONS

	Correct detection	False alarm
Visit	$B-\mathcal{L}_c\cdot e^{-\frac{\mathrm{P}_i^D}{1-\mathrm{P}_i^D}}$	$-\mathcal{L}_c\cdot e^{-\frac{\mathrm{P}_i^D}{1-\mathrm{P}_i^D}}$
Not visit	$-B$	0

expected payoff $u_n(b_i)$ for not visiting b_i can be respectively expressed as

$$u_v(b_i)=[B-\mathcal{L}_c\cdot e^{-\frac{\mathrm{P}_i^D}{1-\mathrm{P}_i^D}}]\cdot\mathrm{P}_i^D+[-\mathcal{L}_c\cdot e^{-\frac{\mathrm{P}_i^D}{1-\mathrm{P}_i^D}}]\cdot(1-\mathrm{P}_i^D)$$
$$=B\cdot\mathrm{P}_i^D-\mathcal{L}_c\cdot e^{-\frac{\mathrm{P}_i^D}{1-\mathrm{P}_i^D}}, \quad (8)$$
$$u_n(b_i)=-B\cdot\mathrm{P}_i^D. \quad (9)$$

Since the AUV carries limited energy E_{ini}, its energy consumption should be considered. The current residual energy E_{res} of the AUV at hover point $\mathcal{P}_k$ can be expressed as

$$E_{res}(\mathcal{P}_k)=E_{ini}-\sum_{i=1}^{k-1}\mathcal{L}(\mathcal{P}_i). \quad (10)$$

The energy required for the AUV floating to the surface after collecting the data in b_i can be represented as

$$E_{back}=\mathcal{L}_{float}. \quad (11)$$

We define the ratio of the cruising cost $\mathcal{L}(b_i)$ to $E_{res}-E_{back}$ as

$$\varepsilon_i=\frac{\mathcal{L}(b_i)}{E_{res}-E_{back}}. \quad (12)$$

We consider ε_i in the following cases to evaluate the feasibility of visiting b_i.

- $\varepsilon_i<0$ holds when $E_{res}<E_{back}$. In this case, the AUV has not enough energy to return to the sink, facing the potential of losing the AUV.
- $\varepsilon_i>1$ holds when $\mathcal{L}(b_i)>(E_{res}-E_{back})$, which means the residual energy of the AUV is insufficient to return to the sink when it visits b_i. In this case, b_i should not be visited.
- $\varepsilon_i=0$ holds when $\mathcal{L}(b_i)=0$, which represents that b_i is the current position of the AUV.
- $\varepsilon_i\in(0,1]$ holds when $\mathcal{L}(b_i)<(E_{res}-E_{back})$. In this case, b_i is an effective potential node to visit.

At the current hovering position, the AUV has to choose the next visiting node, at the risk of false alarm error detection, to maximize its payoff considering the data loss and cruising energy consumption. Based on the prior discussion, the detected nodes should satisfy the requirement of $0<\varepsilon\leq 1$. They are the next potential nodes to be visited by the AUV. Denoting $\mathcal{B}$ by the next visiting candidate nodes, the individual-based dynamic trajectory planning (IDTP) problem for the AUV can be formulated as

$$b_i^*=\arg\max_{b_i\in\mathcal{B}}\left[u_v(b_i)+\sum_{b_j\in\mathcal{B},j\neq i}u_n(b_j)\right]. \quad (13)$$

Using (13), the AUV can determine the next moving direction towards node b_j^* to the next hover point $\mathcal{P}_{i+1}$. The current hover point $\mathcal{P}_i$ and the next hover point $\mathcal{P}_{i+1}$ will then form a *track* for the AUV's trajectory. Considering the communication range, the position of node b_i^* is not equivalent to the next hover point $\mathcal{P}_{i+1}$, and the data in the nodes near the track will be collected during the cruise. Once collecting the data from node b_i^*, the AUV will stop at the hover point $\mathcal{P}_{i+1}$ to detect nodes and determine the next trajectory track, considering that the detection performance is better at hovering state than at moving state. The cruise trajectory will be formed dynamically by the consecutive tracks, which can be presented by $\mathcal{P}=\{\mathcal{P}_1,\mathcal{P}_2,\cdots,\mathcal{P}_n\}$.

The nearest node detected will be possibly output by (13). According to the payoff matrix in Tab. II, the nearest node requires the least cruising energy $\mathcal{L}_c$, and will possibly have the largest detection probability P_D since the incident signal at the UCA from the nearest node would be the strongest. In this sense, (13) is similar to the nearest node strategy N-n [18]. The difference is that N-n needs the knowledge of node positions while IDTP uses the detection information.

Notice that multiple nodes may locate in a cruising direction and share the same trajectory in data collection, in which case a cruising trajectory can collect data from multiple nodes. The nearest node strategy in IDTP does not consider the node distribution feature and does not exploit the sharing of trajectory. To further improve the data collection efficiency, we will propose a grouping-based dynamic trajectory planning for the AUV in the next section.

IV. GROUPING-BASED DYNAMIC TRAJECTORY PLANNING FOR AUV DATA COLLECTION

The proposed GDTP includes detection, grouping, and selection phases.

A. Detection Phase

We use a passive detection model to detect the existence of sensor nodes. Multiple signal classification (MUSIC) is first applied to obtain the angles of the $M-1$ incident signals, and then we use a power-based hypothesis to judge the existence of nodes and calculate their detection probabilities.

1) Node direction estimation: MUSIC is used to estimate the direction of nodes. As mentioned before, $(M-1)$ signal sources are incident on the array. The first K incident angles represent the incident directions of the real signal sources, and the last $(M–1–K)$ incident angles are generated by noises. The received signal of UCA is shown in (4). The autocovariance matrix $\mathbf{R}_X$ can be expressed as

$$\mathbf{R}_X=\mathbf{E}[\boldsymbol{X}\boldsymbol{X}^{\mathrm{H}}]$$
$$=\boldsymbol{A}(\theta,\varphi)\mathbf{R}_S\boldsymbol{A}^{\mathrm{H}}(\theta,\varphi)+\sigma^2\boldsymbol{I}_{(M)}, \quad (14)$$

where $\mathbf{R}_S=\mathbf{E}[\mathbf{S}(t)\mathbf{S}^{\mathrm{H}}(t)]$, σ^2 represents the noise variance, and $\boldsymbol{I}_{(M)}$ is a $M\times M$ dimensional identity matrix. The eigen decomposition of $\mathbf{R}_X$ can be expressed

$$\mathbf{R}_X=\boldsymbol{U}\Lambda\boldsymbol{U}^{\mathrm{H}}$$
$$=\boldsymbol{U}_S\Lambda_S\boldsymbol{U}_S^{\mathrm{H}}+\boldsymbol{U}_N\Lambda_N\boldsymbol{U}_N^{\mathrm{H}}, \quad (15)$$

This article has been accepted for publication in a future issue of this journal, but has not been fully edited. Content may change prior to final publication. Citation information: DOI 10.1109/JIOT.2022.3141402, IEEE Internet of Things Journal

where $\boldsymbol{U}$ and Λ are the $M\times(M-1)$ dimensional eigenvector matrix and eigenvalues matrix of $\mathbf{R}_X$ respectively. $\boldsymbol{U}_S$ is the signal subspace, $\boldsymbol{U}_N$ is the noise subspace, and Λ_S and Λ_N are diagonal matrices composed of K large eigenvalues and the remaining small eigenvalues. The MUSIC spatial spectrum [28] can be expressed as

$$P_{MUSIC}=\frac{1}{\boldsymbol{A}^{\mathrm{H}}(\theta,\varphi)\boldsymbol{U}_N\boldsymbol{U}_N^{\mathrm{H}}\boldsymbol{A}(\theta,\varphi)}. \tag{16}$$

The $M-1$ possible source directions are then estimated by the largest $M-1$ peaks on the MUSIC space spectrum.

2) Hypothesis Test for Each Node: The MUSIC algorithm can find directions of all the possible $M-1$ sources. However, it cannot tell which one is the real source or the virtual source. Therefore, We use a hypothesis test to judge the existence of real sources and their detection probabilities. The hypothesis test for the signal power of the $(\hat{\theta}_k,\hat{\varphi}_k)$ is shown as (6). In $H_0(k)$, the received signal obeys $s_k\sim N(0,\sigma^2)$. In $H_1(k)$, the received signal obeys $s_k\sim N(0,(M-1)p_k+\sigma^2)$. The likelihood function ratio can be expressed as [29]

$$\begin{aligned}\Lambda(s_k)&=\frac{p(\mathbf{x};\hat{p}_k;H_1)}{p(\mathbf{x};\sigma^2;H_0)}\\&=\frac{\exp\left[\frac{p_k}{2\sigma^2[(M-1)p_k+\sigma^2]}\sum_{n=1}^{N}\hat{s}_k^2(n)\right]}{\left(\frac{(M-1)p_k}{\sigma^2}+1\right)^{\frac{N}{2}}},\end{aligned} \tag{17}$$

where

$$\hat{s}_k=\boldsymbol{a}_k^{\mathrm{H}}\mathbf{R}^{-1}\mathbf{X}(n)/(\boldsymbol{a}_k^{\mathrm{H}}\mathbf{R}^{-1}\boldsymbol{a}_k),n=1,2,\cdots,N. \tag{18}$$

The log likelihood ratio can be represented as

$$l(s_k)=-\frac{N}{2}\ln\left(\frac{(M-1)p_k}{\sigma^2}+1\right)+\frac{(M-1)p_k}{2\sigma^2[(M-1)p_k+\sigma^2]}\sum_{n=1}^{N}\hat{s}_k^2(n). \tag{19}$$

Suppose that the decision threshold is γ_0, the hypothesis test can be expressed as

$$l(s_k)\underset{H_0(k)}{\overset{H_1(k)}{\gtrless}}\gamma_0. \tag{20}$$

The power-based hypothesis test becomes

$$T(s_k)=\frac{\sum_{n=1}^{N}\hat{s}_k^2(n)}{N}\underset{H_0(k)}{\overset{H_1(k)}{\gtrless}}\gamma_0', \tag{21}$$

where

$$\gamma_0'=\frac{2\sigma^2((M-1)p_k+\sigma^2)}{N(M-1)p_k}\left[\gamma_0+\frac{N}{2}\ln\left(\frac{(M-1)p_k}{\sigma^2}+1\right)\right]. \tag{22}$$

The number of signals $\hat{K}$ is the number of estimated sensor nodes, which equals the number of decisions with $H_1(k),k=1,2,\cdots,M-1$. Moreover, the false alarm probability P^F and the detection probability P^D related to $(\hat{\theta}_k,\hat{\varphi}_k)$ can be given by

$$\mathrm{P}_k^F=\mathrm{P}_r\{T(s_k)>\gamma_0':H_0\}=Q_{\chi_N^2}\left(\frac{\gamma}{\sigma_n^2}\right), \tag{23}$$

and

$$\mathrm{P}_k^D=\mathrm{P}_r\{T(s_k)>\gamma_0':H_1\}=Q_{\chi_N^2}\left(\frac{\gamma}{Mp_k+\sigma_n^2}\right), \tag{24}$$

respectively. $Q_{\chi_N^2}(x)$ is the right-tailed distribution of the random variable χ_N^2 that obeys the chi-square distribution.

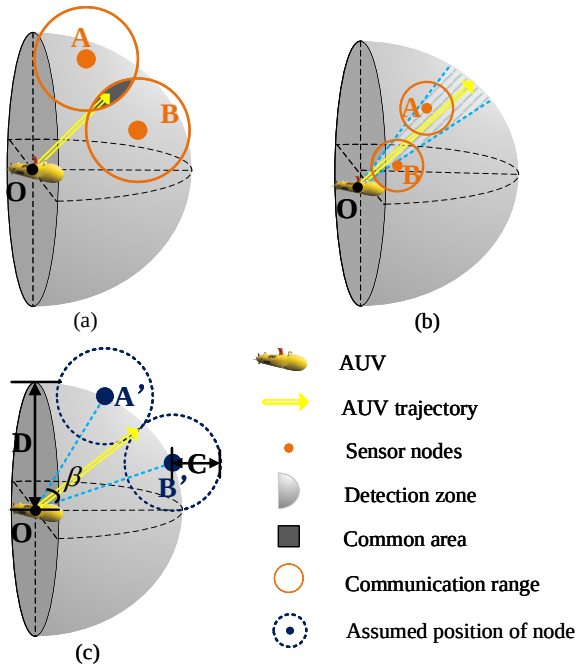

Fig. 5. Common area model. The sector A'OB' is within the communication range of one common track.

B. Grouping Phase

We observe that the AUV can collect multiple nodes' data in one moving track, as shown in Figs. 5(a) and 5(b). Figure 5(a) depicts the scenario when two nodes are not far away from each other. In this case, they share a common communication area. The AUV can collect the data in the two nodes simultaneously by moving to the common area. Alternatively, there is no common area between node A and node B in Fig. 5(b), but they are both near the same track. The AUV can also collect their data in one moving track. In the cases of Figs. 5(a) and 5(b), A and B can be grouped together for one cruising track.

To collect multiple nodes' data in one track, the AUV faces the following problems: *i*) whether there exists such a track to group nodes, and *ii*) how to calculate such a track by using only the estimated angles of nodes.

We propose a common area model to group nodes and calculate the moving direction for the groups. As shown in Fig. 5(c), suppose there are two points A' and B' at the edge of the detection area, and they have a common area. Since the AUV only acquires the direction knowledge of the nodes instead of the distance between them, we group the detected nodes in the area of $A'OB'$. Angle threshold for grouping β can be calculated by

$$\beta=\angle A'OB'=2\mathrm{arc}\sin(\frac{C}{D}), \tag{25}$$

since $\sin(\angle A'OB'/2)=C/D$, where C denotes the communication range and D represents the detection range. For two detected nodes with estimated directions $(\hat{\theta}_i,\hat{\varphi}_i)$ and $(\hat{\theta}_j,\hat{\varphi}_j)$, they will fall into the area of $A'OB'$ and can be grouped if

This article has been accepted for publication in a future issue of this journal, but has not been fully edited. Content may change prior to final publication. Citation information: DOI 10.1109/JIOT.2022.3141402, IEEE Internet of Things Journal

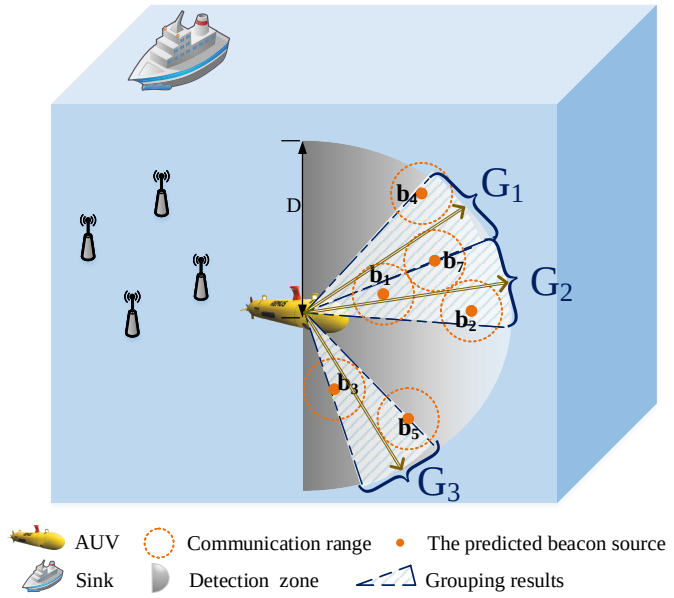

Fig. 6. An example of GDTP grouping. The sensors are divided into three groups according to (26).

their angles satisfy

$$|\hat{\theta}_i - \hat{\theta}_j| < \beta, \text{ and } |\hat{\varphi}_i - \hat{\varphi}_j| < \beta. \tag{26}$$

When any two nodes in G_j satisfy (26), the cruising direction for the track to collect data in G_j is then calculated by

$$\bar{\theta} = \frac{1}{2}\big[\max\{\hat{\theta}, \hat{\theta} \in G_j\} + \min\{\hat{\theta}, \hat{\theta} \in G_j\}\big], \tag{27}$$

$$\bar{\varphi} = \frac{1}{2}\big[\max\{\hat{\varphi}, \hat{\varphi} \in G_j\} + \min\{\hat{\varphi}, \hat{\varphi} \in G_j\}\big]. \tag{28}$$

The proposed GDTP uses (26) to group nodes and uses (27) and (28) to determine the cruising direction of that group.

C. Selection Phase

The detected nodes are divided into multiple groups in the grouping phase, as shown in Fig. 6. The AUV has to choose one group to visit, which can obtain the maximum payoff in data collection.

Similar to the statement in Section III.D, visiting a group can obtain the data from the nodes in that group, while it has a risk of data losses in other groups. Thus, the payoff and loss for visiting a group can be expressed as follows

$$u_v(G_j) = \sum_{i \in G_j} B \cdot \mathrm{P}_i^D - \max_{i \in G_j} \mathcal{L}_c \cdot \exp(-\frac{\mathrm{P}_i^D}{1-\mathrm{P}_i^D}), \tag{29}$$

$$u_n(G_j) = \sum_{i \in G_j} u_n(b_i) = -\sum_{i \in G_j} B \cdot \mathrm{P}_i^D. \tag{30}$$

The AUV should select the following group to visit, having the maximum expected payoff

$$G_j^* = \arg\max_{G_j \in \mathcal{G}} \left[u_v(G_j) + \sum_{G_k \in \mathcal{G}, k \neq j} u_n(G_k) \right]. \tag{31}$$

The AUV can select the group G_j^* using (31), and the next moving direction towards the group G_j^* can be determined using (27) and (28). After collecting the expected sensor's data, the AUV will hover and start the next detection. Alg. 1 summarizes the details of GDTP, and it has a time complexity of $\mathcal{O}(|\mathcal{B}|^2)$.

Algorithm 1 Grouping-based dynamic trajectory planning

Input: The data amount threshold B, the cruise cost of the AUV moving to the detection edge $\mathcal{L}_c$ and angle threshold for grouping β.

Detection Phase:

Sensors broadcast beacons when the sensed data reaches to B.
The AUV estimates $(\hat{\theta}, \hat{\varphi})$ and P_i^D using (16) and (24). Put detected nodes that satisfy $0 < \varepsilon_i \leq 1$ into $\mathcal{B}$.

Grouping Phase:

for i=1 to $|\mathcal{B}|$ **do**
  for j=1 to $|\mathcal{B}|$ **do**
    Calculate $|\hat{\theta}_i - \hat{\theta}_j|$ and $|\hat{\varphi}_i - \hat{\varphi}_j|$.
    if satisfy (26) **then**
      Put b_j into G_i.
    end if
  end for
  Put G_i into $\mathcal{G}$.
end for

Selection Phase:

for all $G_j \in \mathcal{G}$ **do**
  Calculate $u_v(G_j)$ and $u_n(G_j)$ using (29) and (30).
  Calculate $G_j^* = \arg\max_{G_j \in \mathcal{G}} \left[u_v(G_j) + \sum_{G_k \in \mathcal{G}, k \neq j} u_n(G_k) \right]$.
  Find $\bar{\theta}_{G_j^*}$ and $\bar{\varphi}_{G_j^*}$ using (27) and (28).
end for

Output: The direction of the AUV next cruising $(\bar{\theta}_{G_j^*}, \bar{\varphi}_{G_j^*})$.

D. Probe Dead Zone

The AUV may enter into a probe dead zone (PDZ) during its dynamic cruising, where the AUV detects no nodes. In the PDZ, the nodes will go to sleep after reporting their data to the AUV (see Section III.B), and the other nodes are beyond the detection area of the current hover point of the AUV. Without any detected nodes, the AUV cannot determine its next cruising direction by using (13) or (31).

We use a random walk approach for the AUV to escape the PDZ. At a hover point in the PDZ, the AUV randomly chooses a cruising direction and moves along this direction. When nodes are detected during the movement, the AUV will use (31) to determine its next movement. When no nodes are detected, the AUV will stop after moving a maximal distance to randomly choose another direction to cruise.

V. Simulation and Discussion

In the simulations, the nodes are uniformly distributed in a 3-dimensional region, and the detailed parameters are listed in Tab. IV. We compare the performance of the proposed GDTP and IDTP with LSACN [5], PNCS-GHA [5], N-n [18] and Random Walk (RW) algorithm [18]. The similarities

TABLE III
THE POWER DETECTED RESULTS OF FIG. 7

	Signals				Noise										
$\theta(^\circ)$	70	-40	30	80											
$\hat{\theta}(^\circ)$	70	-40	30	80	-57	25	-66	-28	-26	-40	18	27	-58	59	-65
$\varphi(^\circ)$	30	60	-10	80											
$\hat{\varphi}(^\circ)$	30	60	-10	80	69	52	40	56	55	13	43	-51	65	-53	2
Judge	H_1	H_1	H_1	H_1	H_0	H_0	H_0	H_0	H_0	H_0	H_0	H_0	H_0	H_0	H_0
P^D	0.9997	0.9998	0.9998	0.9999	0.8924	0.4142	0.5422	0.8568	0.8698	0.8602	0.9085	0.9357	0.4255	0.5698	0.8859

TABLE IV
SIMULATION PARAMETERS

Parameter	Value
Network size $(L \times W \times H)$	$10 \times 10 \times 6$ km^3
Number of nodes	100-500
Communication range (C)	100-500 m
Detection range (D)	2 km
Number of each node's data packets	100 packets
Unit consumption of AUV $(\mathcal{L}_0)$	8 J/m
AUV initial energy (E_{ini})	1600 kJ
AUV floating to the surface $(\mathcal{L}_{float})$	30 kJ
AUV speed	7.72 m/s
Maximum moving distance for a direction in PDZ	1 km

TABLE V
SIMILARITIES AND DIFFERENCES AMONG ALGORITHMS

Algorithm	Node coordinates	Grouping/Clustering	Path planning
GDTP	Unknown	√	Dynamic
IDTP	Unknown	⌀	Dynamic
PNCS-GHA	Known	√	Static
N-n	Known	⌀	Static
LSACN	Unknown	√	Fixed
RW	Unknown	⌀	Dynamic

and differences between these algorithms are summarized in Tab. V. We compare the performance of the algorithms mentioned above in terms of collection efficiency which is the ratio of the collected data packets to the energy consumption of the AUV.

A. Performance of Node Detection

We set the number of snapshots $N = 30$, the number of UCA elements $M = 16$, and the probability of false alarm $P^F = 0.1$. The four signals incident from $(70^\circ, 30^\circ)$, $(-40^\circ, 60^\circ)$, $(30^\circ, -10^\circ)$ and $(80^\circ, 80^\circ)$, and signal noise ratio are 10 dB, 15 dB, 20 dB and 25 dB respectively.

According to (16), the MUSIC spatial spectrum is shown in Fig. 7. There are four higher peaks that represent four signals and other small peaks generated by noises and multipath interference. The largest $M-1$ largest spectral peaks can be found and listed in Tab. III. Using the power-based hypothesis test (6), the four signals are judged as real signals and their detection probabilities are also computed in Tab. III. Then the $\hat{\theta}$, $\hat{\varphi}$, and P^D of any possible node can be obtained.

It is shown in Tab. III that the detection approach in Section IV.A can obtain the incident directions of the signal sources

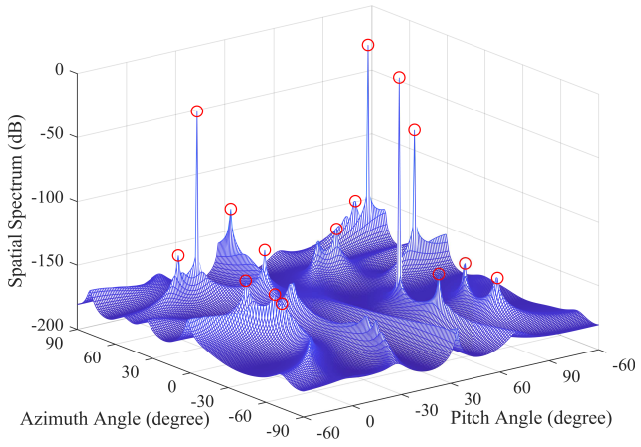

Fig. 7. DOA estimation. Four incident signals can be observed from the MUSIC spatial spectrum in our simulation settings.

and identify each source with a high probability. The results in Tab. III verify the feasibility of the detection approach and the feasibility of our proposed planning-while-detecting framework.

B. An Example of Trajectories

We next show the trajectories of GDTP, IDTP, and the existing PNCS-GHA [5] and N-n algorithm [18] in a two-dimensional plane by assuming that all the nodes are deployed in the same depth. For fair comparison, the AUV has the same energy for different algorithms. Therefore, the trajectory lengths for the four algorithms are the same [6]. As shown in Fig. 8, the trajectories of our proposed IDPT and GDTP algorithms are different from the existing PNCS-GHA and N-n in that our proposed algorithms do not need to visit the positions of nodes to collect data. Fig. 8(a) shows that GDTP can collect more nodes' with the same length of the trajectory. Both IDTP and N-n tend to choose the nearest node as the next target for data collection. As shown in Fig. 8(b), due to the limited number of nodes detected by IDTP while N-n has the positions of all nodes, the trajectories of IDTP and N-n are different. However, they can collect a similar number of nodes' data.

C. Impact of Communication Range

Since the communication range affects the grouping of GDTP as shown in (25), we study the impact of the com-

This article has been accepted for publication in a future issue of this journal, but has not been fully edited. Content may change prior to final publication. Citation information: DOI 10.1109/JIOT.2022.3141402, IEEE Internet of Things Journal

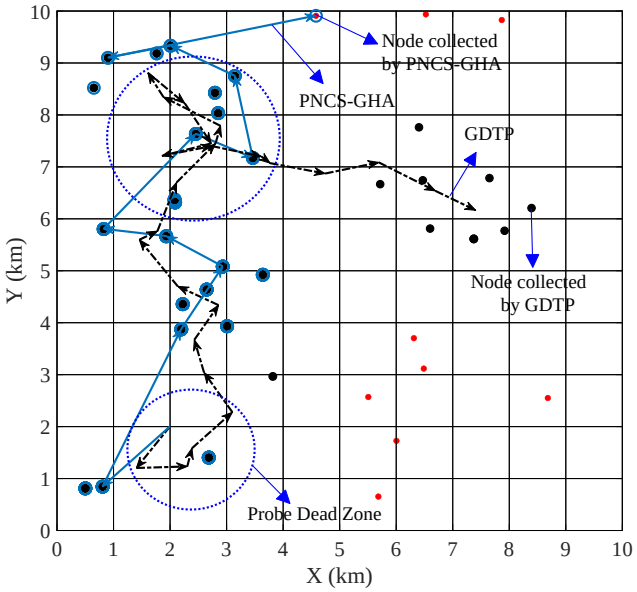

(a) GDTP and PHCS-GHA

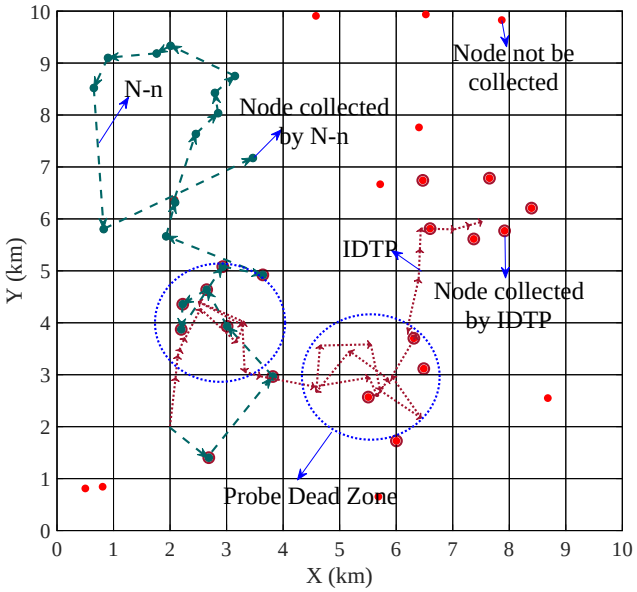

(b) IDTP and N-n

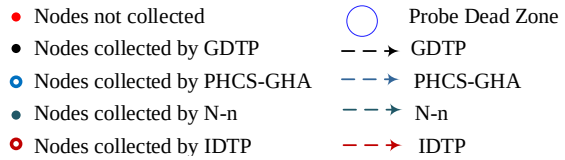

Fig. 8. The trajectories of GDTP, PHCS-GHA, IDTP, and N-n. The detection range is 2 kilometers, and the communication is 1 kilometer.

munication range on GDTP. We use optical links, RF links, and underwater acoustic links to represent the typical communication ranges at 10, 100, and 500 meters in the simulations, respectively.

As shown in Fig. 9, the collection efficiencies of the

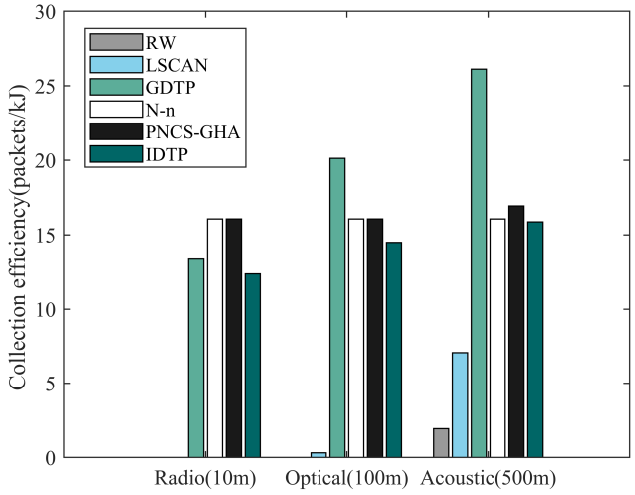

Fig. 9. Collection efficiency at different communication ranges in static scenes

algorithms are increased with the communication range in a static scenario that the node positions are fixed. Our proposed GDTP has a large advantage over the other algorithms as the communication range increases. The reason is that a larger communication range will lead to a larger group by GDTP. Thus, the movement in a track can collect more data. When the communication range is short (e.g., 10 meters), the number of nodes in a group becomes small. In this case, GDTP and IDTP have similar collection efficiencies. Having the knowledge of node positions, N-n and PNCS-GHA can have a higher data collection efficiency than our proposed IDTP. However, the collection efficiency of IDTP increases faster than N-n and PNCS-GHA as the communication range increases. The fixed path planning LSCAN and the random planning RW can hardly visit the node positions when the communication range is short, leading to extremely low collection efficiencies. The N-n algorithm has the same collection efficiency regardless of the changes of the communication ranges, since it always visits the nearest node.

In Fig. 10, we study the data efficiencies of the algorithms in a dynamic scenario that the nodes are moving. We set sensors to move at a random speed of $0-0.5$ m/s (the turtle swims at about a speed of 0.27–0.5 m/s [30]) and a random direction. Since the static N-n and PNCS-GHA algorithms do not apply to the dynamic scenario where the node positions are not available, we only compare GDTP and IDTP with RW and LSCAN. The fixed trajectory planning by RW and LSCAN collects only a few data when the communication range is short at 10 meters and 100 meters in a large sea area of $10\times10\times6$ km^3. GDTP and IDTP can still achieve significantly high data collection efficiencies by using the long-propagation acoustic for sensor detection.

D. Impact of Node density

The increase of the number of nodes in the network will increase the node density when the coverage area of the

This article has been accepted for publication in a future issue of this journal, but has not been fully edited. Content may change prior to final publication. Citation information: DOI 10.1109/JIOT.2022.3141402, IEEE Internet of Things Journal

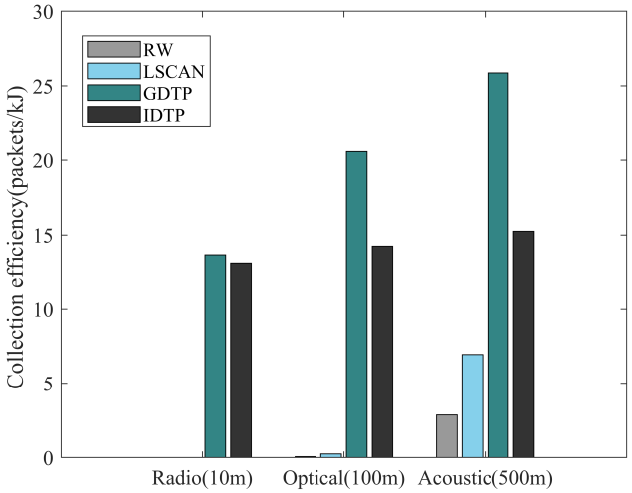

Fig. 10. Collection efficiency at different communication ranges in dynamic scenes

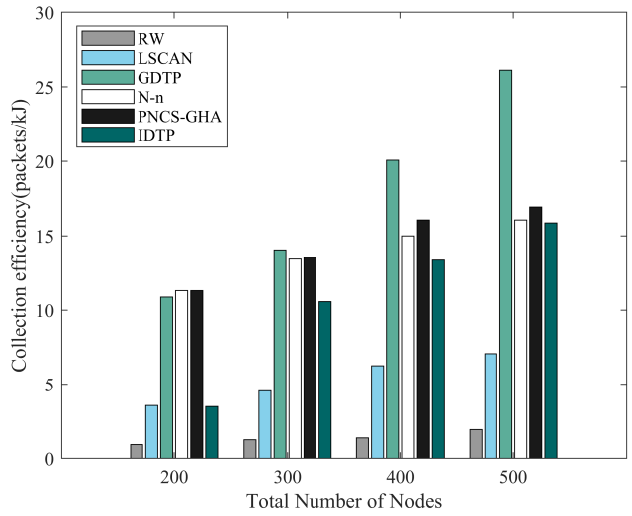

Fig. 11. Collection efficiency at different node densities in static scenes

network is fixed, which has a significant impact on grouping and trajectory planning.

With a communication range of 500 meters, the collection efficiencies of all the algorithms increase with the number of nodes in both the static and dynamic scenes, as shown in Fig. 11 and Fig. 12. This is because as the node density increases, the expected distance between nodes decreases. Thus, the AUV can travel a short distance to visit a node, increasing the collection efficiency. Since the probability of entering into a PDZ becomes small in a dense network, the collection efficiencies of GDTP and IDTP increase faster than the other algorithms as the number of nodes increases. GDTP achieves the highest data collection efficiency in a dense network. The reason beyond is that when the network becomes denser, the number of nodes per group will increase. A visit of a group can then collect more data.

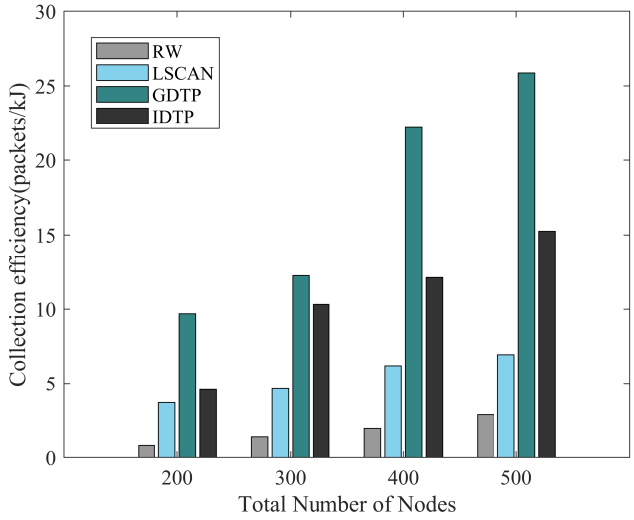

Fig. 12. Collection efficiency at different node densities in dynamic scenes

VI. Conclusion

This paper studied the dynamic path planning problem for the AUV to collect the data in underwater sensors, which can exploit the movement of the AUV to reduce the transmission power of sensor nodes. We considered a scenario that the underwater sensor positions are unavailable for the AUV's trajectory planning, which can be found in typical underwater applications. To address the unavailability of node positions, we proposed a planning-while-detecting framework to dynamically plan the AUV's trajectory. Particularly, we proposed a grouping-based dynamic trajectory planning (GDTP) algorithm, which groups nodes having a common communication area and adjusts the next cruising direction to the group that can collect the largest amount of data at the cost of cruise energy and at the risk of error detection. The simulation results showed that the AUV in GDTP can collect more data with less energy consumption of the AUV in comparison with the existing schemes.

As a future work, we will design an algorithm that exploits the historical detection information and the prior information to plan the trajectory and collect data in a more efficient way.

Mingyue Cheng (Graduate Student Member, IEEE) received the B. Eng. degree in electronic engineering from Nanjing University of Post and Telecommunications, China in 2018. She is currently pursuing the Ph.D. degree in information and communication engineering with the South China University of Technology, Guangzhou, China. Her current research focuses on underwater sensor networks.

Quansheng Guan (S'09-M'11-SM'17) received the B. Eng. degree in electronic engineering from Nanjing University of Post and Telecommunications, China in 2006, and the Ph.D. degree from South China University of Technology (SCUT) in 2011. From 2009 to 2010, he was a visiting Ph.D. student with the University of British Columbia, Canada. From 2012 to 2013, he was a Postdoc Researcher at the Chinese University of Hong Kong. He was a visiting scholar at Singapore University of Technology and Design in 2013, and a visiting professor in Polytech Nantes, France, in 2016. He is currently a full Professor with the School of Electronic and Information Engineering, SCUT. His research interests include wireless communications and networking, underwater acoustic networking, fog/cloud computing, and networked interactions and economics.

Dr. Guan is the co-recipient of Best Paper Awards from IEEE ICCC 2014 and IEEE ICNC 2016, and Best Demo Award from ACM WUWNET 2018. He was a guest editor for Mobile Information System, and currently associate editors for IEEE Access and Int. J. Distributed Sensor Networks. He has been a TPC member for numerous conferences, and a reviewer for peer-reviewed journals and conferences.

Fei Ji (M'06) received the B.S. degree in applied electronic technologies from Northwestern Polytechnical University, Xi'an, China, and the M.S. in bioelectronics and Ph.D. degrees in circuits and systems both from South China University of Technology, Guangzhou, China, in 1992, 1995, and 1998, respectively. She was a Visiting Scholar with the University of Waterloo, Canada, from June 2009 to June 2010. She worked in the City University of Hong Kong as a Research Assistant from March 2001 to July 2002 and a Senior Research Associate from January 2005 to March 2005.

Dr. Ji is currently a Professor with the School of Electronic and Information Engineering, South China University of Technology. She was the Registration Chair and the Technical Program Committee (TPC) member of IEEE 2008 International Conference on Communication System. Her research focuses on wireless and underwater acoustic communication systems and networking.

Julian Cheng (S'96–M'04–SM'13) received the B.Eng. degree (Hons.) in electrical engineering from the University of Victoria, Victoria, BC, Canada, in 1995, the M.Sc.(Eng.) degree in mathematics and engineering from Queens University, Kingston, ON, Canada, in 1997, and the Ph.D. degree in electrical engineering from the University of Alberta, Edmonton, AB, Canada, in 2003. He is currently a Full Professor in the School of Engineering, Faculty of Applied Science, The University of British Columbia, Kelowna, BC, Canada. He was with Bell Northern Research and NORTEL Networks. His current research interests include machine learning and deep learning for wireless communications, optical wireless technology, and quantum communications. He was the Co-Chair of the 12th Canadian Workshop on Information Theory in 2011, the 28th Biennial Symposium on Communications in 2016, and the sixth EAI International Conference on Game Theory for Networks (GameNets 216). He currently serves as an Area Editor for the IEEE TRANSACTIONS ON COMMUNICATIONS, and he was a past Associate Editor of the IEEE TRANSACTIONS ON COMMUNICATIONS, the IEEE TRANSACTIONS ON WIRELESS COMMUNICATIONS, the IEEE COMMUNICATIONS LETTERS, and the IEEE ACCESS. Dr. Cheng served as a Guest Editor for a Special Issue of the IEEE JOURNAL ON SELECTED AREAS IN COMMUNICATIONS on Optical Wireless Communications. He is also a Registered Professional Engineer with the Province of British Columbia, Canada. Currently he serves as the President of the Canadian Society of Information Theory as well as the Secretary for the Radio Communications Technical Committee of IEEE Communications Society.

Yankun Chen received the master and Ph.D. degree in 2009 and 2018 in school of Electronic and Information Engineering at the South China University of Technology, Guangdong, China. She now works for South China Sea Marine Survey and Technology Center and is a member of Key Laboratory of Technology for Safeguarding of Marine Rights and Interests and Application. Her main interests are underwater acoustic networks, MAC protocol performance analysis, the simulation of underwater acoustic networks and physical oceanography.

REFERENCES

[1] M. Jahanbakht, W. Xiang, L. Hanzo, and M. R. Azghadi, "Internet of underwater things and big marine data analytics—a comprehensive survey," *IEEE Commun. Surveys Tuts.*, pp. 1–1, 2021. Early access.

[2] C. Kao, Y. Lin, and G. Wu, "A comprehensive study on the internet of underwater things: Applications, challenges, and channel models," *Sensors*, vol. 17, no. 7, pp. 1477–1497, June 2017.

[3] J. Luo, Y. Chen, M. Wu, and Y. Yang, "A survey of routing protocols for underwater wireless sensor networks," *IEEE Commun. Surveys Tuts.*, vol. 23, no. 1, pp. 137–160, 2021.

[4] M. Al-Bzoor, E. Al-assem, L. Alawneh, and Y. Jararweh, "Autonomous underwater vehicles support for enhanced performance in the internet of underwater things," *Trans. Emerg. Telecommun. Technol.*, vol. 32, no. 3, pp. 1–19, Jan. 2021.

[5] G. Han, S. Li, and C. Zhu, "Probabilistic neighborhood-based data collection algorithms for 3D underwater acoustic sensor networks," *IEEE Sensors J.*, vol. 17, no. 2, pp. 1–16, Feb. 2017.

[6] G. Han, S. Shen, and H. Song, "A stratification-based data collection scheme in underwater acoustic sensor networks," *IEEE Trans. Veh. Technol.*, vol. 67, no. 11, pp. 10 671–10 682, Nov. 2018.

[7] Y. Chen and Y. Lin, "Mobicast routing protocol for underwater sensor networks," *IEEE Sensors J.*, vol. 13, no. 2, pp. 737–749, Feb. 2013.

[8] N. Ilyas and T. A. Alghamdi, "AEDG: Auv-aided efficient data gathering routing protocol for underwater wireless sensor networks," *Procedia Comput. Sci.*, vol. 52, no. 1, pp. 568–575, June 2015.

[9] K. Jawaad and C. Ho-Shin, "Data-gathering scheme using auvs in large-scale underwater sensor networks: A multihop approach," *Sensors*, vol. 16, no. 10, pp. 1–19, Oct. 2016.

[10] G. Han and X. Long, "An auv location prediction-based data collection scheme for underwater wireless sensor networks," *IEEE Trans. Veh. Technol.*, vol. 68, no. 6, pp. 6037–6049, June 2019.

[11] G. Han, X. Long, and C. Zhu, "A high-availability data collection scheme based on multi-auvs for underwater sensor networks," *IEEE Trans. Mobile Comput.*, vol. 19, no. 5, pp. 1010–1022, May 2019.

[12] G. A. Hollinger, "Underwater data collection using robotic sensor networks," *IEEE J. Sel. Areas Commun.*, vol. 30, no. 5, pp. 899–911, June 2012.

[13] X. Zhuo, M. Liu, and Y. Wei, "Auv-aided energy-efficient data collection in underwater acoustic sensor networks," *IEEE Internet of Things Journal*, vol. 7, no. 10, pp. 10 010–10 022, Oct.2020.

[14] R. Duan, J. Du, and C. Jiang, "Value based hierarchical information collection for auv enabled internet of underwater things," *IEEE Internet Things J.*, vol. 7, no. 10, pp. 9870–9883, Oct. 2020.

[15] C. Cheng and L. Li, "Data gathering problem with the data importance consideration in underwater wireless sensor networks," *J. Netw. Comput. Appl.*, vol. 78, pp. 300–312, Jan. 2017.

[16] H. Nam, "Data-gathering protocol-based auv path-planning for long-duration cooperation in underwater acoustic sensor networks," *IEEE Sensors J.*, vol. 18, no. 21, pp. 8902–8912, Nov. 2018.

[17] E. M. Arkin, S. P. Fekete, and J. S. Mitchell, "Approximation algorithms for lawn mowing and milling," *Computational Geometry*, vol. 17, no. 1-2, pp. 25–50, 2000.

[18] W. Gong and M. Li, "Comparison of heuristics for resolving the traveling salesman problem with information technology," *Advanced Materials Research*, vol. 886, pp. 593–597, 2014.

[19] G. Han, S. Shen, H. Wang, J. Jiang, and M. Guizani, "Prediction-based delay optimization data collection algorithm for underwater acoustic sensor networks," *IEEE Trans. Veh. Technol.*, vol. 68, no. 7, pp. 6926–6936, July 2019.

[20] S. Basagni, L. Boloni, and P. Gjanci, "Maximizing the value of sensed information in underwater wireless sensor networks via an autonomous underwater vehicle," in *Proc. IEEE INFOCOM, Toronto*, May 2014, pp. 988–996.

[21] J. Yan, X. Yang, X. Luo, and C. Chen, "Energy-efficient data collection over auv-assisted underwater acoustic sensor network," *IEEE Syst. J.*, vol. 12, no. 4, pp. 3519–3530, Dec. 2018.
[22] C. Lv, F. Yu, M. Zhu, and S. Xiao, "Auv real-time dynamic obstacle avoidance strategy based on relative motion," *Eng. Lett.*, vol. 27, no. 1, pp. 234–240, Feb. 2019.
[23] T. Riedl and A. Singer, "Towards a video-capable wireless underwater modem: Doppler tolerant broadband acoustic communication," in *Proc. IEEE UCOMMS, Sestri Levante, Italy*, Sept. 2014, pp. 1–5.
[24] R. Khalil, M. Babar, and T. Jan, "Towards the internet of underwater things: Recent developments and future challenges," *IEEE Consum. Electron. Mag.*, pp. 1–1, 2020. Early access.
[25] X. Han, M. Liu, S. Zhang, and Q. Zhang, "A multi-node cooperative bearing-only target passive tracking algorithm via uwsns," *IEEE Sensors Journal*, vol. 19, no. 22, pp. 10 609–10 623, Nov. 2019.
[26] Z. Li, S. Li, J. Jia, and D. Ju, "Doa estimation of underwater wideband signals based on improved omp method," in *OCEANS 2019 - Marseille*, June 2019, pp. 1–6.
[27] J. Jiang, Y. Du, and P. Wei, "Detection of the number of sources based on power estimation," in *Proc. ICCCAS, Chengdu*, vol. 2, Nov. 2013, pp. 278–282.
[28] R. Schmidt, "Multiple emitter location and signal parameter estimation," *IEEE Trans. Antennas Propag.*, vol. 34, no. 3, pp. 276–280, March 1986.
[29] T. Yardibi and J. Li, "Source localization and sensing: A nonparametric iterative adaptive approach based on weighted least squares," *IEEE Trans. Aerosp. Electron. Syst*, vol. 46, pp. 425–436, Jan. 2010.
[30] C. Kinoshita, T. Fukuoka, T. Narazaki, Y. Niizuma, and K. Sato, "Analysis of why sea turtles swim slowly: a metabolic and mechanical approach," *J. Exp. Biol.*, vol. 224, no. 4, pp. 1–11, Feb. 2021.